Available online at www.sciencedirect.com

ScienceDirect

ARTICLE

High Speed Imaging Observation on Molten Bridge of AgSnO₂ Electrical Contact Material

Chen Jinghong,   Chen Song,   Li Muyang,   Xie Ming,   Ren Xianli

State Key Laboratory of Advanced Technologies for Comprehensive Utilization, Kunming Institute of Precious Metals, Kunming 650106, China

Abstract: An electrical contact-high speed imaging experimental system was developed to study the basic characteristics and laws of molten bridges of AgSnO₂ electrical contact material. On the one hand, the quantitative measurements were investigated by high speed imaging technology. On the other hand, the microstructure and element distribution on the surface of contacts were analyzed by SEM and EDS after molten bridges behavior. Results indicate that the evolution behavior of molten bridges of AgSnO₂ contacts can be divided into three regimes: the initial melting period, a stable period and an unstable period during which it eventually ruptures. Molten bridges and arc can exist simultaneously in which there is some cooperation and competition relationship. The dimension of molten bridges of AgSnO₂ contact material is micron scale, the diameter of molten bridges increases with the increase of current and the length decreases with the increase of current. In the process of the evolution behavior of molten bridges, the feature of molten bridges can be divided into three types: the pier, follow by the cylindrical and the dumbbell. The morphology and element distribution of the contacts surface are changed by the behavior of molten bridges.

Key words: molten bridge; high speed imaging; arc; AgSnO₂ electrical contact material

Ag/MeO materials are widely researched and used in the field of electrical contact materials[1,2]. Silver tin oxide (AgSnO₂) is an alloy in which the SnO₂ particles are dispersed in Ag matrix, and it is a kind of nontoxic and environment-friendly electrical contact materials which has been developed rapidly in recent years[3]. It was found that AgSnO₂ had become a focus of investigations in electrical contact materials and a possibility to replace AgCdO due to its excellent properties such as better welding resistance, comparably low material migration with low contact resistance, less arc erosion and long life time[4-11]. In the process of contacts separation, the actual contact area decreases with the decrease of contact pressure, the contraction effect of current increases sharply, and the Joule heat causes the contact area to soften, deform and even melt so that the molten bridge comes into being under the surface tension of the metal liquid[12,13]. Not only will molten bridges lead to the transfer of contact materials but

also their rupture will greatly affect saturated vapor pressure in the contact gap and arc life. And some new researches also deem that molten bridges may be one of the main reasons causing the separation of contact welding[14-16]. Up to now, the direct observation of molten bridges has some challenges due to its small dimension (micron to millimeter scale) and short existence time (microsecond to millisecond level)[17]. Research on the behavior of molten bridges has always been an important basic issue in the electrical contact subject, so it is significant to study the behavior of molten bridges of AgSnO₂ electrical contact material[18]. The molten bridge can be divided into dark bridge and glow bridge[19,20]. The dark bridge is a molten bridge which is in the state of heat balance during the slow separation of the contact pair. Not only doesn't the glow bridge meet the thermal equilibrium conditions but also it is not easy to be observed and recorded. The dark molten bridge was mainly studied in this paper.

In order to further study the characteristics and influence factors of the molten bridge behavior, to improve the reliability, accuracy and service life of the switch contacts, the electrical contact-high speed imaging experimental system was designed by ourselves for the study on the behavior of molten bridges of $AgSnO_2$ electrical contact material. It is able to study the physical phenomena occurring in the high speed dynamic process of $AgSnO_2$ contacts through the analysis and comparison of the captured image [21]. The microstructure and element distribution of the contacts surface were analyzed by scanning electron microscope (SEM) and energy dispersion spectrum (EDS) analysis after the behavior of molten bridges. Thus, in turn, the behavior of molten bridges was investigated. In the range of 5 A to 25 A load current, the contact voltage is 0.35 V while the molten pool and molten area appear by the calculation of φ-θ theory [22] on pure Ag contacts. In order to observe the molten bridge more clearly, the experimental conditions were adopted for 6 V (8, 10, 12, 15, 18, 20 A), a total of 6 sets of conditions, the $AgSnO_2$ contact samples were studied under the DC and single split mode with the electrical contact-high speed imaging experimental system.

1 Experiment

Ag and Sn powders with purity of more than 99% were prepared by powder metallurgy process to make $AgSnO_2$ (the content of SnO_2 was 8wt%) material used in experiment [23]. The shape of the upper contacts was made into conical and the lower ones was made into cylindrical by cutting, grinding, polishing and cleaning preparation shown in Fig. 1.

The electrical contact-high speed imaging experimental system consists of four parts, which are the light, the JF04C electrical contact testing machine, the imaging system and the computer shown in Fig. 2. JF04C electrical contact testing machine was used to test the contact samples under the DC and single split mode. The breaking speed was 50.0 mm/s (v=50.0 mm/s) and the contact force was 50.0 cN (f=50.0 cN). The experimental conditions were 6 V (8, 10, 12, 15,
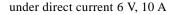
18, 20 A), a total of 6 sets of conditions, and under each condition, 50 electrical contact tests were conducted on the contact samples. Among them, the upper contact was the anode; and the lower one was the cathode. The shooting rate of the high speed camera used in the experiment was 480 fps (N=480 fps), the optical magnification of the camera lens was 50 times and the pixel of the imaging apparatus was 224×160. Before the experiment, the lens group and high speed camera were adjusted to focus, so that the contact samples could be clearly imaged. And the imaging should be the biggest by regulating the objective lens of high speed camera. Then the high speed camera was transferred to the high speed shooting mode to capture the video data of contacts during moving process. The data was transmitted to computer, which was captured by the high speed camera. Then typical images were disposed and selected by EDIUS6.0 software. Diameter and length of molten bridges were determined through EDIUS6.0. According to the exact value of the lower contacts diameter was 1.08 mm, and the diameter and length of molten bridges were gauged by the image measuring software (Digimizer). Finally, the microstructure and element distribution of the contacts surface were analyzed by SEM and EDS after the behavior of molten bridges.
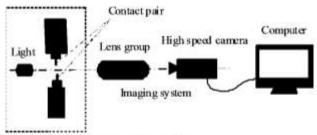
2 Results and Analysis

2.1 High speed imaging observation on the behavior of molten bridges

2.1.1 Observation on the behavior of molten bridges under direct current 6 V, 8 A

Fig. 3a shows the moving track of the contract pair during the closing process but not in contact. As is shown in Fig. 3b, there is a stable molten bridge with approximately cylindrical shape between the contact pair. Between the contact pair, palpable arc is observed in Fig. 3c. According to the diameter of the lower contact 1.08 mm, the diameter of molten bridge measured in Fig. 3a is 0.135 mm, and the length is 0.089 mm.

2.1.2 Observation on the behavior of molten bridges under direct current 6 V, 10 A

Fig. 1   Shape of contact pair samples

Fig. 2   Electrical contact-high speed imaging experimental system

Fig. 3 Observation on the behavior of molten bridges under direct current 6 V, 8 A: (a) without contact, (b) stable molten bridge, and (c) palpable arc (*v*=50.0 mm/s, *f*=50.0 cN, *N*=480 fps)

Fig. 4a shows that a stable molten bridge with approximate cylindrical shape exists between the contact pair. Fig. 4b illustrates that the molten bridge is broken and obvious arc appears on the right of the contact pair, and there is still a narrow residual molten bridge on the left of arc. In Fig. 4c, the contact pair are in complete separation and the molten bridge and arc are both gone. According to the diameter of the lower contact 1.08 mm, the diameter of molten bridge measured in Fig. 4a is 0.191 mm, and the length is 0.083 mm.

2.1.3 Observation on the behavior of molten bridges under direct current 6 V, 12 A

In Fig. 5a, an approximate dumbbell shaped molten bridge is observed between the contact pair. Fig. 5b illustrates that the molten bridge is broken and obvious arc appear on the left of the contact pair, and there is still a small amount of residual molten bridge on the right of the contact pair. Between the contact pair, there is an approximate cylindrical molten bridge in Fig. 5c. According to the diameter of the lower contact 1.08 mm, the diameter of molten bridge measured in Fig. 5c is 0.222 mm, and the length is 0.085 mm.

2.1.4 Observation on the behavior of molten bridges under direct current 6 V, 15 A

Fig. 6a illustrates that there is a stable molten bridge with approximate cylindrical shape between the contact pair. Between the contact pair, large amounts of arc are observed

in Fig. 6b. As is shown in Fig. 6c, clear arc exists in the middle of the contact pair, while residual molten bridges appear both on the right and left side of arc, and there is a tiny molten bridge remaining in the middle of arc. According to the diameter of the lower contact 1.08 mm, the diameter of molten bridge measured in Fig. 6a is 0.261 mm, and the length is 0.087 mm. In the same way, the diameters of molten bridges in Fig. 6c are 0.036 mm (left) and 0.027 mm (right).

2.1.5 Observation on the behavior of molten bridges under direct current 6 V, 18 A

Between the contact pair, there is an approximate dumbbell shaped molten bridge in Fig. 7a. As is shown in Fig. 7b, dazzling arc are observed between the contact pair. Fig. 7c shows that a stable molten bridge with approximate cylindrical shape exists between the contact pair. According to the diameter of the lower contact 1.08 mm, the diameter of the molten bridge measured in Fig. 7c is 0.277 mm, and the length is 0.079 mm.

2.1.6 Observation on the behavior of molten bridges under direct current 6 V, 20 A

In Fig. 8a, there is a molten bridge between the contact pair. As is shown in Fig. 8b, great deals of arc are observed between the contact pair. Fig. 8c illustrates that the contact pair are in complete separation and the molten bridge and arc

Fig. 4 Observation on the behavior of molten bridges under direct current 6 V, 10 A: (a) stable molten bridge, (b) molten bridge break, and (c) complete separation of the molten bridge and arc (*v*=50.0 mm/s, *f*=50.0 cN, *N*=480 fps)

Fig. 5   Observation on the behavior of molten bridges under direct current 6 V, 12 A: (a) approximate dumbbell shaped molten bridge,
(b) molten bridge break (obvious arc appears on the left), and (c) approximate cylindrical molten bridge (v=50.0 mm/s, f=50.0 cN,
N=480 fps)

Fig. 6   Observation on the behavior of molten bridge under direct current 6 V, 15 A: (a) stable molten bridge with approximate cylindrical
shape, (b) large amounts arc, and (c) clear arc in the middle (v=50.0 mm/s, f=50.0 cN, N=480 fps)

Fig. 7   Observation on the behavior of molten bridges under direct current 6 V, 18 A: (a) approximate dumbbell shaped molten bridge,
(b) dazzling arc, and (c) stable molten bridge with approximate cylindrical shape (v=50.0 mm/s, f=50.0 cN, N=480 fps)

Fig. 8   Observation on the behavior of molten bridges under direct current 6 V, 20 A: (a) a molten bridge, (b) great deals of arc, and (c) the
contact pair are in complete separation and the molten bridge and arc (v=50.0 mm/s, f=50.0 cN, N=480 fps)

are both gone. According to the diameter of the lower contact
1.08 mm, the diameter of molten bridge measured in Fig.8a
is 0.295 mm, and the length is 0.076 mm.

2.2   Analysis on the observation results of molten bridges behavior

The evolution behavior of the molten bridge of AgSnO$_2$

contacts can be divided into three regimes: the initial melting period, a stable period and an unstable period during which it eventually ruptures. This conclusion is consistent with the research result of P. Koren[24]. It can be observed from the experiment that the shape of the molten bridge is pier rough in its initial formation stage, then the shape develops into cylindrical type with the increase of breaking distance of contact pair, and the shape becomes dumbbell when the molten bridge is in the period of instability until its rupture. This is consistent with the conclusions of P. M. Davidson[25] that the form of the molten bridge can be divided into three types: the pier, the cylindrical and the dumbbell. The diameter of the molten bridge of $AgSnO_2$ contacts ranges from 0.027 mm to 0.295 mm and the size of length is between 0.076 and 0.089 mm. This is consistent with the existing research that the dimension of precious metal molten bridge is micron grade [26].

Fig.9 illustrates the relationship between the diameter and length of molten bridges of $AgSnO_2$ contacts and the current. It can be perceived from the graph that although there are some fluctuations in the experimental data, the overall trend is that the diameter of the molten bridge increases with the increase of current, and the length of the molten bridge decreases with the increase of current. The results of this paper are consistent with the results of H. Ishida[27] on Pd contacts and K. Miyanaga[28] on Al contacts.

Table 1 shows the ratio relation of the diameter and current of the molten bridge during the stable period. The mean ratio between diameter and current ($a=d/I$) is 0.0148 mm/A. The result of T. Utsumi [29] for the calculation on pure Ag contacts is 0.0424 mm/A and the result of J. J. Lander[30] for the calculation on pure Ag contacts is 0.0390 mm/A. These results belong to one order of magnitude and the figure in this paper is smaller compared with those. This is mainly due to, that in the process of forming the molten pool, SnO_2 will float to the surface of the molten pool and cover on the Ag matrix thus playing an impeditive role on the formation of the molten bridge. Thus, the diameter of the molten bridge of $AgSnO_2$ is smaller than that of pure Ag contacts under the same current condition and $AgSnO_2$ contacts have better resistance to material transfer and other excellent electrical contact performance.

In the experiment, we can observe that molten bridges and arc can exist simultaneously, which is seldom reported in previous literature. There are some cooperation and competition relationship between molten bridges and arc. The cooperative relationship is mainly shown in the appearance of arc when molten bridges are broken, which illustrates that molten bridges can assist in the production of arc. The competition relationship is mainly manifested that molten bridges and arc cannot coexist in the same place, molten bridges and arc exist inevitably in different positions and there is a certain distance apart when they emerge simultaneously.
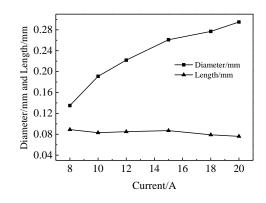

Fig.9   Relationship of the diameter and length of molten bridges of $AgSnO_2$ contacts to the current

Table 1 Relationship between diameter and current of molten bridge

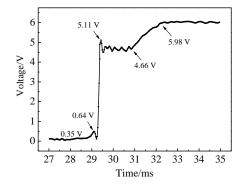| Diameter, d/mm	Current, I/A	a/mm·A^{-1}
0.135	8	0.0169
0.191	10	0.0191
0.222	12	0.0185
0.261	15	0.0174
0.277	18	0.0154
0.295	20	0.0015

Fig.10   Voltage-time characteristics of the corresponding Fig.6c (6 V, 15 A, v=50.0 mm/s, f=50.0 cN)

The voltage-time oscillogram during the contact separation of Fig.6c is shown in Fig.10. The real contact area decreases when the contact pair has just started to separate. At this point, the voltage is slightly increased and the contact area begins to melt. With the separation of the contact pair, molten bridges appear and small amounts of arc are followed. So the voltage oscillogram shows a trend of decrease after the initial increase (from 0.35 V to 0.64 V and then to 0 V). With the increase of the breaking distance, most of molten bridges disconnect and the voltage sharply increases. When

the voltage reaches over 5.11 V, substantial arc appears and the voltage decreases. And the voltage waveform of an approximate platform (4.66 V) is presented. With the further increase of the breaking distance, the voltage increases slowly until the 6 V is reached and then remains unchanged. In this process, the arc is gone until the contact pair is completely disconnected.

2.3 SEM observation on contacts after the behavior of molten bridges

2.3.1 SEM observation on anode contact after the behavior of molten bridges

Fig.11 shows the SEM morphology of the $AgSnO_2$ anode contact (upper contact) after the behavior of molten bridges. The molten region can be observed at the top of the anode contact from Fig.11. It is observed that the molten region is composed of a large number of overlapping molten spots, which indicates that there are massive molten pools in the process of experiment.

Fig.12 shows the morphologies of the concretionary molten pools in the molten region of the $AgSnO_2$ anode contact. These molten pools are round and their surfaces are relatively flat. Obvious splash particles are not observed during the solidification of molten pools, which is mainly concerned with the behavior of molten bridges. The diameters of these molten pools are 0.111, 0.038, 0.0589
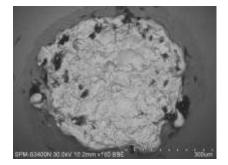
and 0.0376 mm. It can be considered that the diameters of the molten bridges which develop into the molten pools are not greater than that of the molten pools. This is basically consistent with the data observed by high speed imaging. EDS analysis shows that the distribution of Sn is comparatively symmetrical in different molten pools, and the content is about 6 wt%.

2.3.2 SEM observation on cathode contact after the behavior of molten bridges

Fig.13 shows SEM morphologies of the $AgSnO_2$ cathode contact (lower contact) after the behavior of molten bridges. The molten region can be observed in the central part of the cathode contact from Fig.13a. It is observed that the molten region is composed of a large number of overlapping molten spots in Fig.13b.

Fig.14 shows the morphologies of the concretionary molten pools in the molten region of the $AgSnO_2$ cathode contact. The molten pools are approximately round and obvious splash particles are not observed during the solidification of molten pools. Their surfaces are sunken which are mainly related to the impact of molten pools by the falling molten bridges after the fast rupture of molten bridges. The diameters of molten pools in Fig.14a and Fig.14b are 0.012 and 0.0319 mm, respectively, which are approximately consistent with the data observed by high speed imaging. However, the overlaps between molten pools are obvious and large particles can be found in the edge of some molten pools. EDS analysis shows that the distribution of Sn is comparatively symmetrical in different molten pools, and the content is about 6 wt%.

2.4 Analysis on SEM observation

The evolution behavior of the molten bridges can affect the surface morphology and distribution of $AgSnO_2$ contacts. The appearance of approximate circular molten pools is mainly related to the behavior of molten bridges. The basic properties of molten pools include that the inner structure of molten pools is composed of Ag rich phase and SnO_2 rich phase. Most of the SnO_2 phase will float to the surface of molten pools and cover on the Ag matrix. The diameters of

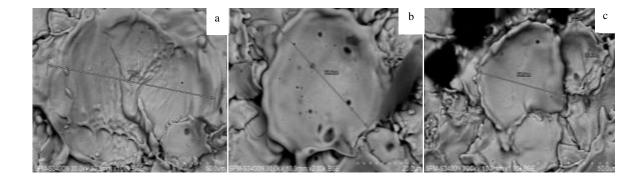Fig.11   SEM morphology of anode contact after molten bridges behavior

Fig.12   Molten pools morphologies of anode contact with different diameters of molten pools: (a) 0.111 mm; (b) 0.038 mm; (c) 0.0589 and 0.0376 mm
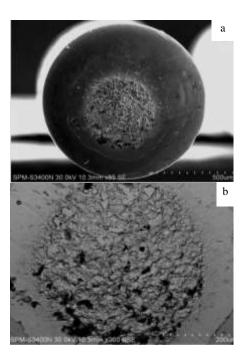
Fig. 13   SEM morphologies of cathode contact after molten bridges behavior
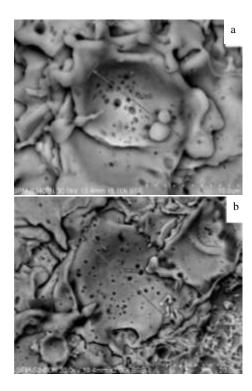

Fig. 14   Molten pools morphologies of cathode contact with diameters of molten pools of 0.012 mm (a) and 0.0319 mm (b)

molten bridges are no larger than that of molten pools which verifies that the dimension of molten bridges of AgSnO$_2$ contacts is micron scale. At the same time, the shapes of

molten bridges are the pier, the column and the dumbbell in the process of their evolution behavior which can be verified by the figure of the molten pools is approximately circular.

3   Conclusions

1) The evolution behavior of molten bridges of AgSnO$_2$ contacts can be divided into three regimes: the initial melting period, a stable period and an unstable period during which it eventually ruptures.

2) The molten bridge and arc phenomenon can exist simultaneously, which is seldom reported in previous literatures. There are some cooperation and competition relationship between molten bridges and the arc.

3) The molten bridge of AgSnO$_2$ contact material is micron scale. The diameter of the molten bridge increases with the increase of current; the length decreases with the increase of current. The reason the AgSnO$_2$ contact material is better than the pure Ag contact material is illustrated from the view of the dimension of molten bridges.

4) In the process of the evolution behavior of molten bridges, the shape of the bridge can be divided into three types: the pier, follow by the cylindrical and the dumbbell. The morphology and element distribution of the contact surface are changed by the behavior of molten bridges.

References

1   Shen Y S. *IEEE Trans*[J], 1986, 9(6): 71
2   Wang Haitao, Wang Jingqin, Du Jiang *et al*. *Rare Metal Materials and Engineering*[J], 2014, 43(8): 1846
3   Zhang Qi, Ye Fan, Huang Xiwen *et al*. *Rare Metal Materials and Engineering*[J], 2015, 44(5): 1293 (in Chinese)
4   Wang Song, Zheng Tingting, Xie Ming *et al*. *Rare Metal Materials and Engineering*[J], 2014, 43(4): 796
5   Wingler J, Sumption A. *Rare Metals*[J], 2010, 29(3): 248
6   Liu X M, Wu S L, Chu P K. *Materials Chemistry and Physics* [J], 2006, 98(2-3): 477
7   Zheng Ji, Li Songlin, Dou Fuqi *et al*. *Rare Metals*[J], 2009, 28(1): 19
8   Liu Linjing, Chen Jingchao, Feng Jing *et al*. *Rare Metal Materials and Engineering*[J], 2011, 40(5): 935 (in Chinese)
9   Jeannot D, Pinard J, Ramoni P. *IEEE Transactions on Components Packaging and Manufacturing Technology*[J], 1994, 17(1): 17
10   Lu J G, Wang J Q, Zhao J Y. *Rare Metals*[J], 2002, 21(4): 289
11   Boettcher R D. *Arcing Failure of ROHS Compliant Electromagnetic Relays*[D]. Maryland: University of Maryland, 2012
12   Chen Z K, Witter G J. *IEICE Transactions on Electronics*[J], 2004, 87(8): 1248
13   Li Zhenbiao, Xu Jinling, Huang Liang *et al. Electrical and Energy Management Technology*[J], 2007, 5: 1 (in Chinese)
14   Zhao L J, Li Z B, Zhang H S *et al. IEICE Transactions on Electronics*[J], 2011, 94(9): 1362
15   Yamano S, Sugimoto H, Sone H *et al. Proceedings of the*

　　Fortieth IEEE Holm Conference on Electrical Contacts[C].
　　Holm: IEEE, 1994: 89

16　Slade P G, Hoyaux M F. *IEEE Transactions on Parts, Hybrids and Packaging*[J], 1972, 8(1): 35

17　Liu Jinyou, Wang Qian, Yang Xiaocheng *et al. Electrical Engineering Materials*[J], 2014, (6): 29 (in Chinese)

18　Holm R. *Electrical Contacts, Theory and Applications*[M]. Fourth Editions, New York: Springer, 1967

19　Ishida H, Taniguchi M, Hideaki S *et al. IEICE Transactions on Electronics*[J], 2005, 88(8): 1566

20　Utsumi T. *IEEE Transactions on Parts, Materials and Packaging*[J], 1969, 5(1): 62

21　Zhang Sanxi, Yao Min, Sun Weiping. *High Speed Imaging and Its Application Technology*[M]. Beijing: National Defence Industry Press, 2006 (in Chinese)

22　Llewellyn Jones F. *The Physics of Electrical Contacts*[M]. Oxford: The Clarendon Press, 1957

23　Xie Ming, Wang Song, Fu Zuoxin *et al. Electrical Engineering Materials*[J], 2013(2): 36 (in Chinese)

24　Koren P, Nahemow M, Slade P G. *IEEE Transactions on Parts, Hybrids, and Packaging*[J], 1975, 11(1): 4

25　Davidson P M. *British Journal of Applied Physics*[J], 1954(5): 189

26　Cheng Lichun. *Electrical Contact Theory and Its Application*[M]. Beijing: China Machine Press, 1989 (in Chinese)

27　Ishida H, Suzuki S, Hideaki S *et al. IEICE Transactions on Electronics*[J], 2006, 89(8): 1136

28　Miyanaga K, Kayano Y, Takagi T *et al. IEICE Transactions on Electron*[J], 2009, E92-C(8): 1020

29　Utsumi T. *IEEE Trans on Parts, Material and Packing*[J], 1969, PMO-5(1): 62

30　Lander J J, Germer L H. *Journal of Applied Physics*[J], 1948, 19(10): 910

$AgSnO_2$ 电接触材料熔桥行为的高速摄像研究

陈静洪，陈　松，李幕阳，谢　明，任县利

(昆明贵金属研究所 稀贵金属综合利用新技术国家重点实验室，云南 昆明 650106)

摘　要：以 $AgSnO_2$ 电接触材料为研究对象，借助高速摄像技术并与电接触试验机组成电接触-高速摄像试验体系，观测触头熔桥行为的基本特征和规律，并进行定量测量，同时通过扫描电镜 (SEM) 和能谱 (EDS) 分析对熔桥行为后触头表面的微观结构和元素分布进行分析。结果表明，$AgSnO_2$ 触头熔桥演化行为可分为接触区域熔化、熔桥稳定存在和熔桥失稳及断开3个阶段，熔桥和电弧现象可以同时存在，并且存在一定的协同和竞争关系，$AgSnO_2$ 触头材料的熔桥尺寸为微米级，熔桥直径随电流的增大而增大，熔桥长度随电流的增大而减小。熔桥演化行为过程中熔桥形状依次表现为墩粗型、圆柱型和哑铃型，熔桥行为会改变触头的表面形貌和元素分布。

关键词：熔桥；高速摄像；电弧；$AgSnO_2$ 电接触材料

作者简介：陈静洪，男，1990 年生，硕士生，昆明贵金属研究所稀贵金属综合利用新技术国家重点实验室，云南 昆明 650106，电话：0871-8328841，E-mail: hellochenjh@163.com